Heat Flux from Flames to Vertical Surfaces

J. G. Quintiere and T. G. Cleary.
Quintiere is with the University of Maryland, and Cleary is with the National Institute of Standards and Technology, Gaithersburg, Maryland.

Abstract

Dimensional analysis is used to examine heat transfer from flames to vertical surfaces. Configurations include a line fire against a wall, a square burner flame against a wall and in a corner, and window flames impinging on a wall. Dimensionless parameters that affect flame heat flux include x/l_f, y/D, l_f/D, and kD where x is vertical distance, y is horizontal distance, l_f is flame length, D is burner dimension, and k is the flame absorption coefficient. Only the effect of these variables is shown. No general correlation is developed, and more data are needed before these results can be applied with confidence.

Introduction

An understanding of, and ability to predict, the heat flux from flames is critical to assessing the ignition and flame spread of materials. Current models for both phenomena rely on knowing the heat flux from the flame. In general, it is not currently practical to predict the heat flux from flames, since this depends on the flame configuration and properties, with radiation playing a more complex role than convection. Hence, it might be more practical, albeit limited, to seek correlations for flame heat flux in terms of the configuration and fuel properties.

This paper presents a preliminary analysis of flame heat flux for several configurations. It will consider dimensional analysis to represent concisely the significant dimensionless variables that affect flame heat flux. The configurations here consist of a line fire against a wall or a wall fire, a square burner flame against a wall or in a corner, and window flames impinging on a wall.

The first case has been experimentally studied by Orloff *et al.*,[1,2] Ahmad and Faeth,[3] Quintiere *et al.*,[4] and Harkleroad.[5] A correlation has been developed for the case of flames of limited height (less than 2 m). Mitler[6] has developed a theoretical basis for the correlation. These results will be reviewed.

The second case represents a typical fire scenario used in the standard room fire tests being considered by ASTM and ISO. Limited flame heat transfer experimental studies have been conducted by Babrauskas *et al.*,[7,8] Janssens,[9] Janssens and Tran,[10] Williamson *et al.*,[11] and Cleary.[12]

Fire Technology, Vol 30, No. 2, 209-231, 2nd Quarter, 1994

The third case has been studied by Oleszkiewicz,[13,14] who used a propane-fed burner in a compartment to generate a window flame. He varied both the fire energy release rate and the window size. As in all the previous investigations cited, Oleszkiewicz measured the heat flux with commercially available heat flux transducers that record the total (convective and radiative) incident heat flux to a cold target. No effect of the heated wall in which the "cold" sensors were imbedded has been taken into account, and the measurements are considered to be steady. The flux was measured at several points along a wall above the window on the centerline.

This study attempts to integrate these data for each configuration by using dimensionless variables. The data are too limited to develop general correlations at this time, but trends can be discerned in terms of the dimensionless variables. Future work is indicated to further develop the results into more useful correlations.

Theoretical Basis for Analysis

To develop the correlation forms from dimensional analysis, we begin with the incident flame heat flux, given as

$$\dot{q}'' = \dot{q}_c'' + \dot{q}_r'' \tag{1}$$

where the convective component is given by

$$\dot{q}_c'' = h\left(T_f - T_\infty\right) \tag{2}$$

and the radiative component is given by

$$\dot{q}_r'' = \sigma T_f^4\left(1 - e^{-\kappa l_m}\right) \tag{3}$$

Here, we have employed the mean beam length approximation l_m to characterize the radiative flux to the boundary of the fire. The flame temperature is denoted by T_f and the target temperature by T_∞, while h is the convective heat transfer coefficient, and σ is the Stefan-Boltzmann constant.

We make Equation (1) dimensionless in the following manner:

$$\frac{\dot{q}''}{\sigma T_f^4} = \frac{h}{\sigma T_f^3}\left(1 - \frac{T_\infty}{T_f}\right) + \left(1 - e^{-\kappa l_m}\right) \tag{4}$$

The heat transfer coefficient h is a function of position and the fluid properties in general. The mean beam length l_m is a function of the geometry of the flame. For flames against surfaces, the mean beam length will depend on the nature of the fire. It will be

related to the characteristic flame dimension associated with the direction of radiation to the surface.

For a wall flame or flame due to a line burner, we estimate

$$l_m \leq 2\delta \tag{5}$$

where δ is the boundary layer thickness. This is based on an optically thin infinite slab approximation. The soot region should increase with the fluid dynamic boundary layer as the fire increases in size, making the radiative component increase.

For burner flames against walls where D is a dimension of a side,

$$\frac{l_m}{D} = function\left(\frac{l_f}{D}\right) \tag{6}$$

where l_f is the flame height. For example, Orloff and de Ris[2] consider a flame aspect ratio η to characterize the l_m/D for radiant heat flux to the base of a pool fire flame. For an axisymmetric pool fire, $\eta = \dot{Q}'' / \dot{Q}'''D$ where $\dot{Q}''$ is the energy release rate per unit fuel area and $\dot{Q}'''$ is the energy release rate per unit volume assumed to be constant for turbulent flames. By the relationships, area $\propto D^2$ and volume $\propto l_f D^2$ for this flame, then $\eta \propto l_f/D$. This suggests that l_m/D is a universal function of l_f/D for a given flame configuration. In other words, for a pool fire with respect to heat transfer to the base, we have the result of Orloff and de Ris;[2] for the square burner fire with heat transfer to the wall, we would have another functional relationship. For a flame approximated by a rectilinear parallelepiped with a dimension D on two sides and 4 D high and for radiation to the 1 x 4 side, l_m/D=0.82.[15]

For a window flame of width W_0 and height H_0, we assume that

$$\frac{l_m}{r_0} = function\left(\frac{l_f}{r_0}\right) \tag{7}$$

where r_0 is defined as an equivalent radius of the upper half of the window given by[16,17]

$$r_0 = \sqrt{\frac{H_0 W_0}{2\pi}} \tag{8}$$

or we can define an equivalent diameter consistent with Equation (6) as $D=2\,r_0$.

In general, T_f varies with position in the flame. But for axisymmetric fires, T_f is approximately 800°C for moderate size fires (D~1 m),[18] independent of the fuel, along the centerline for the continuous flame region. In general, the centerline temperature

correlates as a universal function of $x/Q^{*2/5}D$ where $Q^* \equiv \dot{Q}/\rho_\infty c_p T_\infty \sqrt{gD^{5/2}}$. This corresponds to x/l_f since $l_f/D\,\dot{Q}^{*2/5}$, for the most part, in axisymmetric fires. All of this suggests that the temperature and heat flux from flames should roughly depend on flame length, and l_f would be a suitable scale factor for x. Hence, $h/\sigma T_f^3$ and T_∞/T_f should be functions of x/l_f for the most part. Let us consider $T_f=(T_f/T_\infty)T_\infty$ and rewrite Equation (4) as

$$\frac{\dot{q}''}{\sigma T_\infty^4} = \left(\frac{T_f}{T_\infty}\right)^4 \left[\frac{h}{\sigma T_f^3}\left(1-\frac{T_\infty}{T_f}\right)+\left(1-e^{-\kappa l_m}\right)\right]$$

Since κl_m can be represented as κD times some function of l_f/D, $f(l_f/D)$, for a given flame configuration, the following heat flux dependence can be considered:

$$\frac{\dot{q}''}{\sigma T_\infty^4} = \frac{h}{\sigma T_f^3}\left(\frac{T_\infty}{T_f}-1\right)+\left(1-e^{-\kappa D f(l_f/D)}\right) \qquad (9a)$$

or

$$\frac{\dot{q}''}{\sigma T_\infty^4} = function\left(\frac{x}{l_f}, \frac{y}{D}, \frac{l_f}{D}, \kappa D\right) \qquad (9b)$$

Here, D is a characteristic fire dimension significant with respect to radiant heat transfer to the wall. For the line fire, it is related to the boundary layer thickness; for the square burner, it is the side dimension; and for the window, it is the equivalent diameter.

Analysis of Data

Except for the data on line fires and square burners against walls, all of the available heat flux data to be considered in this section have been prescribed in dimensional form (see Tables 1, 2, and 3). That is, the investigators presented the surface heat flux as a function of burner energy release rate and position. Heat flux measurement uncertainty on the order of 10% can be expected in the tabulated data. Here, we attempt to present the results in terms of x/l_f and the other variables indicated in Equation (9b) to seek some generalizations of the data.

Case 1: Line Fire

The geometry for the line fire case is shown in Figure 1. Tu and Quintiere[19] have

TABLE 1
Flat Wall Heat Flux Data Along Centerline Due to a 0.28m Square Burner for Propane[12]

$\dot{Q}$ (kW)	l_f (m)	x (m)	Heat Flux (kW/m²)
50	0.66	0.39	42
		0.69	17
		1.3	4.2
200	1.14	0.39	78
		0.69	56
		1.9	7.2

correlated the average flame height from experiments on combustible solids and obtained

$$l_f = 0.0667\left(\frac{\dot{Q}}{W}\right)^{2/3} \tag{10}$$

where W is the width of the fire and $\dot{Q}$ is the rate of energy release. Both l_f and W are in meters, and $\dot{Q}$ is measured in kW. To make this expression dimensionless, we do the following:

$$\frac{l_f}{W} = \frac{0.0667}{W}\left(\frac{\dot{Q}}{W}\right)^{2/3}$$

$$= \frac{0.0667}{W}\left(\frac{\dot{Q}}{W^{5/2}}\frac{\rho_\infty c_p\sqrt{g}T_\infty}{\rho_\infty c_p\sqrt{g}T_\infty}\right)^{2/3} \tag{11}$$

and specifying ρ_∞=1.1 kg/m³, c_p=1.0 kJ/kg K, g=9.81 m/s², T_∞=298K

$$\frac{l_f}{W} = 6.81Q^{*2/3} \tag{12}$$

where Q^* is defined in terms of the W dimension instead of D, as previously given.

TABLE 2
Corner Wall Heat Flux Data Due to a Square Burner from Various Sources

Fuel	D (m)	Q (kW)	l_f (m)	x (m)	y/D	Heat Flux (kW/m²)	Source
Propane	0.305	41.0	0.781	0.90	0.500	11.5	Janssens (1991)
						13.3	
						12.5	
				1.5		5.30	
						8.30	
						7.80	
		99.0	1.41	0.90		41.0	
				1.5		31.0	
		157	1.91	0.90		55.0	
						56.0	
						57.0	
				1.5		62.0	
						60.0	
						59.0	
	0.300	40.0	0.768	0.20		50.0	Williamson *et al.* (1991)
					0.330	45.0	
				0.70	0.500	20.0	
				0.75		14.0	
					0.330	17.0	
					0.670	10.0	
				1.2	0.500	5.00	
				2.0		3.00	
		150	1.86	0.20		60.0	
					0.330	55.0	
				0.70	0.500	58.0	
					0.330	55.0	
					0.670	35.0	
				1.2	0.500	50.0	
				2.0		55.0	
	0.280	50.0	0.930	0.08 3	0.300	82.0	Cleary (1989)
				0.39	0.540	40.0	

TABLE 2 (cont.)

Fuel	D (m)	Q̇ (kW)	l_f (m)	x (m)	y/D	Heat Flux (kW/m²)	Source
					0.890	24.0	
				0.69	0.540	28.0	
					0.300	40.0	
					0.890	13.0	
				1.3	0.540	10.0	
					0.300	17.0	
				1.9	0.300	6.50	
					0.890	3.50	
	0.490	200	1.62	0.083	0.170	120	
					0.900	37.0	
				0.39	0.310	105	
					0.510	60.0	
					0.900	30.0	
				0.69	0.310	72.0	
					0.510	45.0	
					0.900	22.0	
				1.3	0.310	43.0	
					0.900	12.0	
					0.170	53.0	
				1.9	0.510	14.0	
					0.170	35.0	
Natural gas	0.305	40.0	0.768	1.8	0.500	4.00	Janssens and Tran (1992)
				1.5		5.00	
				1.2		7.00	
				.092		9.60	
				0.61		16.0	
				0.31		32.0	
				1.8		27.0	
				1.5		35.0	
				1.2		38.0	
				0.92		41.0	
				0.61		46.0	
				0.31		52.0	

TABLE 3
Facade Heat Flux Due to a Window Fire Plume[13]

W_0 (m)	H_0 (m)	Q (kW)	x (m)	Heat Flux (kW/m²)	$l_f$exp (m)
0.94	2.0	5500	2.5	44	5.0
			3.5	12	5.0
			4.5	8	5.0
			5.5	4	5.0
		6900	2.5	59	6.0
			3.5	18	6.0
			4.5	10	6.0
			5.5	5	6.0
		8600	2.5	75	7.0
			3.5	26	7.0
			4.5	16	7.0
			5.5	8	7.0
	2.7	5500	3.2	19	
			4.2	6	
			5.2	4	
			6.2	2	
		6900	3.2	35	
			4.2	10	
			5.2	6	
			6.2	3	
		8600	3.2	53	6.2
			4.2	16	6.2
			5.2	10	6.2
			6.2	5	6.2
		10300	3.2	68	
			4.2	16	
			5.2	10	
			6.2	5	
2.6	1.4	5500	1.9	25	3.9
			2.9	23	3.9
			3.9	13	3.9
			4.9	11	3.9

TABLE 3 (cont.)

W_0 (m)	H_0 (m)	$\dot{Q}$ (kW)	x (m)	Heat Flux (kW/m²)	$l_f$exp (m)
		6900	1.9	53	4.4
			2.9	33	4.4
			3.9	17	4.4
			4.9	16	4.4
		8600	1.9	104	5.1
			2.9	59	5.1
			3.9	51	5.1
			4.9	28	5.1
		10300	1.9	209	6.4
			2.9	122	6.4
			3.9	104	6.4
			4.9	57	6.4
	2.0	5500	2.5	11	
			3.5	5	
			4.5	5	
			5.5	3	
		6900	2.5	17	4.5
			3.5	9	4.5
			4.5	7	4.5
			5.5	5	4.5
		8600	2.5	30	5.0
			3.5	15	5.0
			4.5	13	5.0
			5.5	8	5.0
		10300	2.5	43	5.5
			3.5	21	5.5
			4.5	16	5.5
			5.5	10	5.5
	2.7	5500	3.2	7	
			4.2	3	
			5.2	2	
			6.2	1	

TABLE 3 (cont.)

W_0 (m)	H_0 (m)	$\dot{Q}$ (kW)	x (m)	Heat Flux (kW/m²)	$l_f$exp (m)
		6900	3.2	11	5.2
			4.2	5	5.2
			5.2	4	5.2
			6.2	3	5.2
		8600	3.2	17	5.9
			4.2	8	5.9
			5.2	6	5.9
			6.2	4	5.9
		10300	3.2	29	6.2
			4.2	13	6.2
			5.2	9	6.2
			6.2	6	6.2

Results from previous experimental studies are shown in Figures 2a, 2b, and 3 for line and wall fires of gaseous and solid fuels. Results show that the heat flux to wall surfaces starts at low values at the origin, rises rapidly to 20 to 30 KW/m^2, is nearly constant in that range up to $0.5l_f$, then drops off sharply. These results hold for a wide range of heat release rate per unit area (40 to 800 kW/m^2) for flames up to 2 m high. In these figures, the experimental values of flame length were used instead of the results computed by Equation (12). However, the flame lengths should be similar since Equation (12) was developed with data from the same apparatus used to gather the data presented in Figure 3.

Case 2a: Square Burner Against Wall

Cleary[12] conducted limited experiments to measure the heat flux to a wall from a propane burner flame. Flame heights were not recorded. The geometry for this case is shown in Figure 4. Hasemi and Tokunaga[22] correlated flame lengths for this case and obtained

$$\frac{l_f}{D} = CQ^{*2/5} \qquad (13)$$

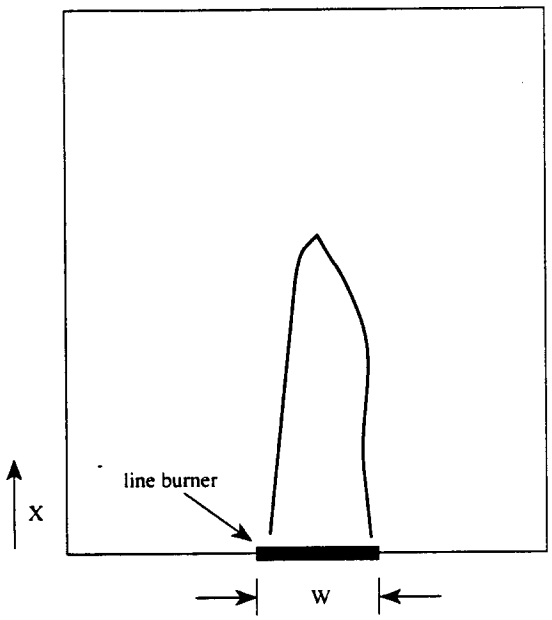

Figure 1. Line fire configuration.

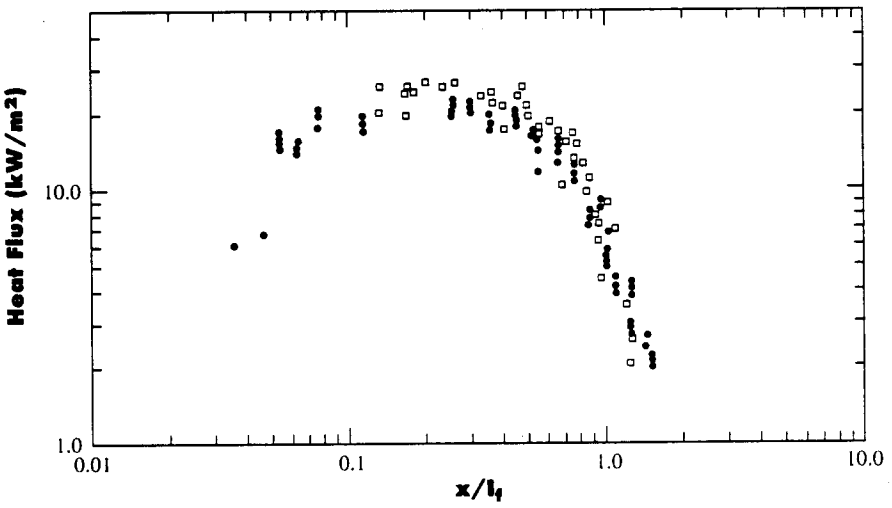

Figure 2a. Wall heat flux due to wall fires. The solid symbols are for a methane line burner fire,[20] and the open symbols are for liquid saturated wall fires.[3]

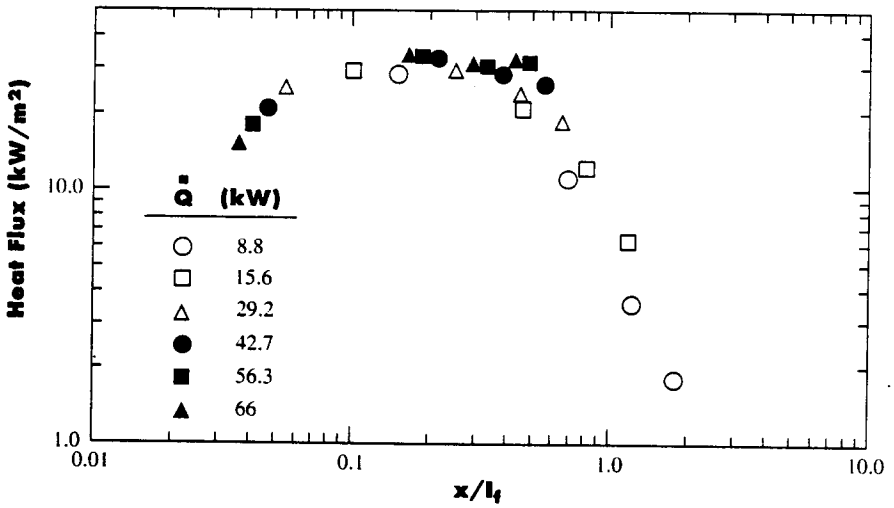

Figure 2b. Wall heat flux due to propane line burner.[22]

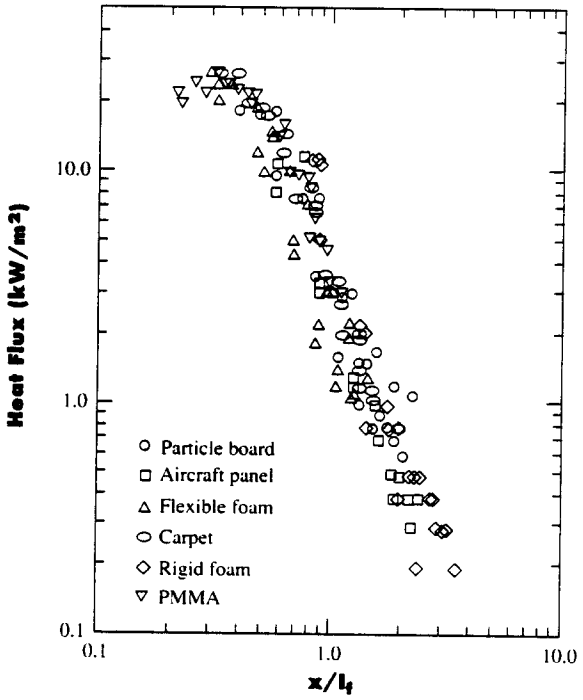

Figure 3. Wall heat flux due to burning wall materials.[4]

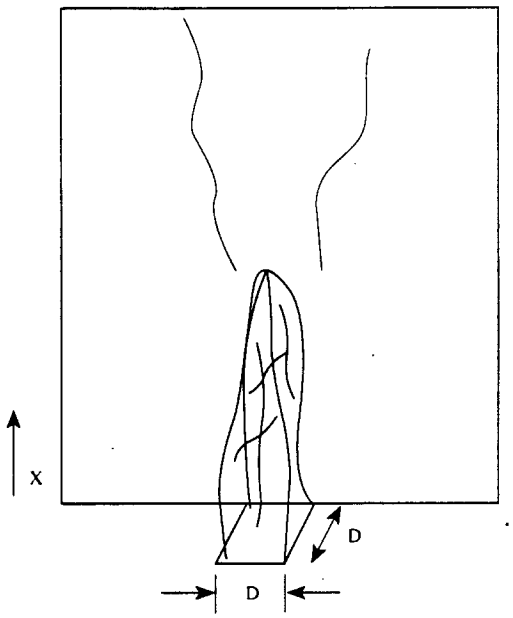

Figure 4. Square burner against a wall.

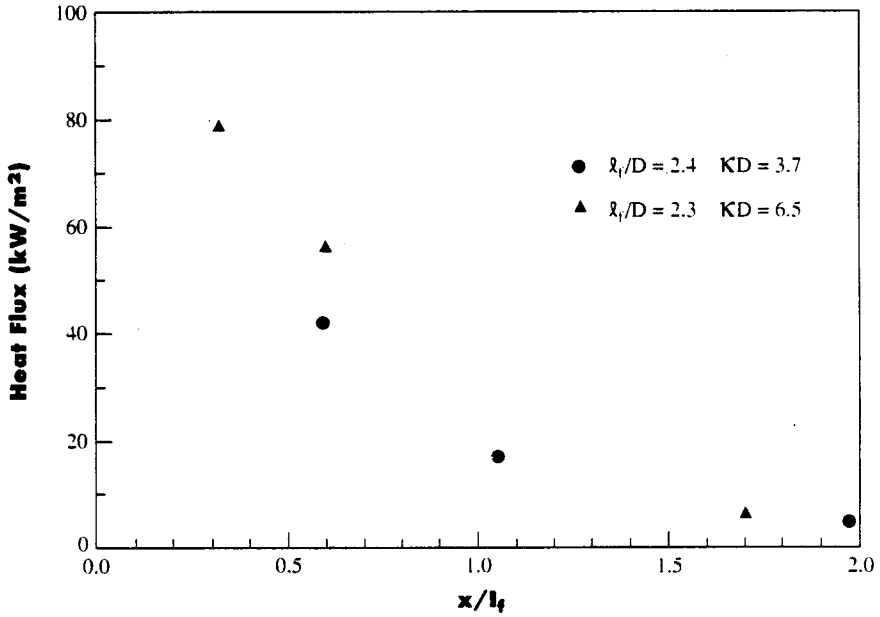

Figure 5. Wall heat flux due to a square burner.[12]

They found that C=2.2 for the continuous flame height and C=3.5 for the flame tips. The data are tabulated in Table 1. Figure 5 shows the heat flux results of Cleary[12] as a function of x/l_f with l_f computed as the continuous flame length. Although l_f/D is nearly constant for these data, the various symbols indicate different burner sizes, thus different κD where κ was taken as 13.3 m^{-1} for propane flames.[15] One would expect that, as κD increases, $\dot{q}''$ would increase, and, at an x/l_f of approximately 0.6, this is seen in Figure 5. More data on corner fires appear to support this argument, as we shall see below, but additional data are needed to more accurately quantify these trends.

Case 2b: Square Burner in a Corner

A number of investigators measured heat flux for a square burner in a corner. Since they were motivated by the proposed ASTM standard room fire test, which considers 40 and 160 kW ignition sources, however, each study is over a limited range of energy release rate. The burners varied in size but were of a similar matrix porous construction to allow the gaseous fuel to be distributed over the surface. All the studies use a similar inert wall material and measure total heat flux to several specific locations with commercial heat flux transducers, presumably based on either the Gardon or the thermopile principle. The sensors were cooled at or near ambient temperature.

Williamson *et al.*[11] measured results along the burner centerline, as well as off axis. They also showed the effect of burner displacement from the wall. We will only consider results for the burner flush with the corner. Janssens and Tran[10] and Cleary[12] obtained similar results using propane as a fuel. Janssens[9] used natural gas. κ for natural gas flames was taken as 6.45 m^{-1}.[15]

Flame height was not measured in any case, so we resort to a computed flame length to examine the data in terms of Equation (9). The geometry for this case is shown in Figure 6. Hasemi and Tokunaga[20] correlated flame heights for a corner fire with the following:

$$\frac{l_f}{D} = CQ^{*2/3} \tag{14}$$

where C=4.3 for flame tips and C=3.0 for the continuous flame region. We computed the continuous flame length. The data and calculated flame heights are presented in Table 2. Figure 7 presents centerline heat flux, where the centerline is defined as position y=$D/2$, as a function of normalized position, and l_f/D. Since D was fixed at 0.3 m, variations in l_f/D are due to changes in the supply rate of propane. As l_f/D increases, the corner flame heat flux appears to become more uniform at 60 kW/m^2 over the flame region. This suggests that, if radiation is the principal component, the flame configuration is becoming thicker over the flame length as l_f/D increases.

Figure 8 shows how heat flux varies with lateral distance from the corner. Limited data are available, but there is clearly an increase in the heat flux as y/D approaches

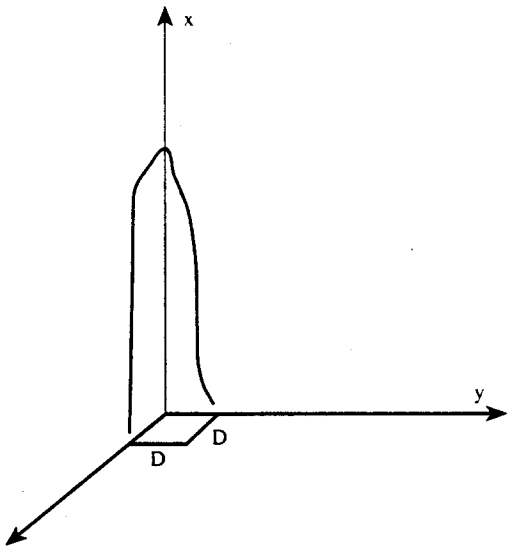

Figure 6. Square burner in a corner.

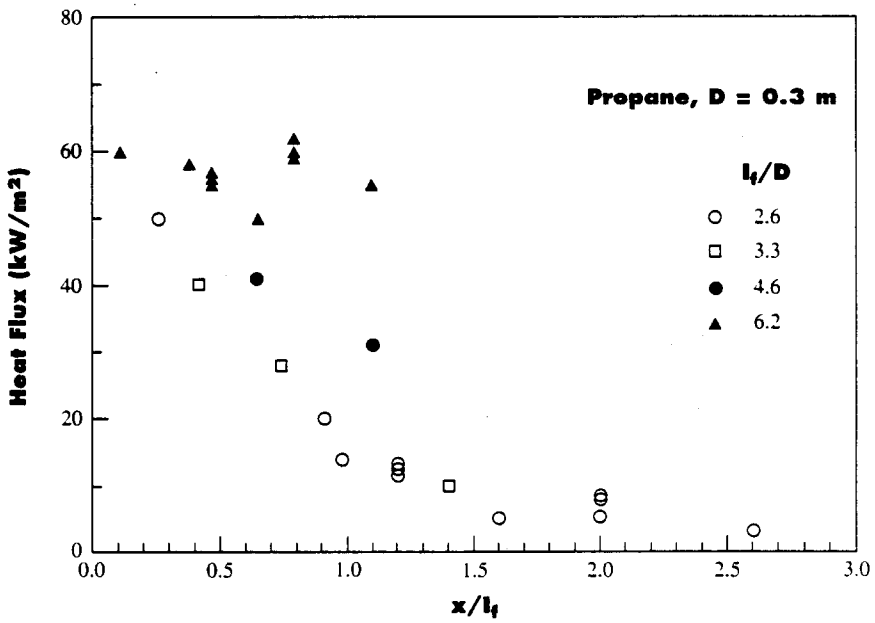

Figure 7. Corner centerline heat flux (effect of energy release rate). Data from Janssens,[9] Williamson *et al.*,[11] and Cleary.[12]

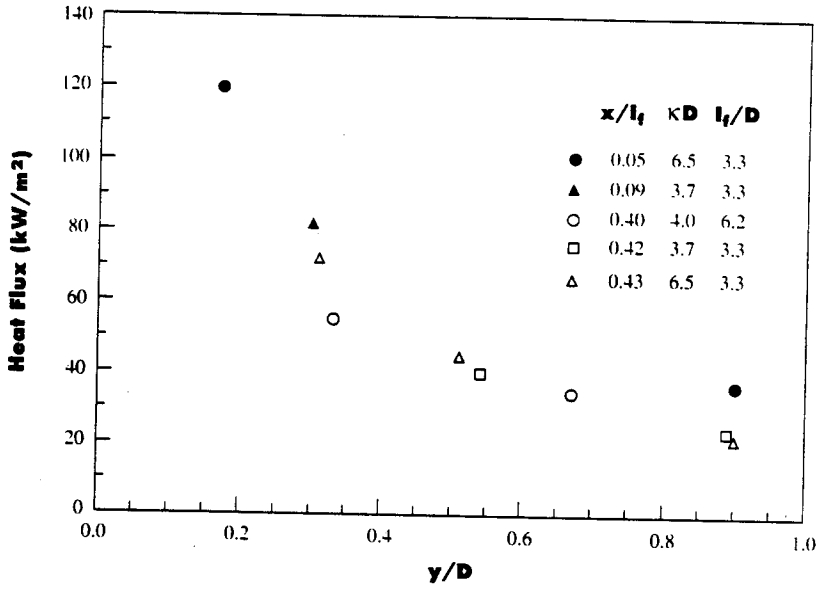

Figure 8. Corner heat flux (effect of distance from corner). Data from Williamson *et al.*[11] and Cleary.[12]

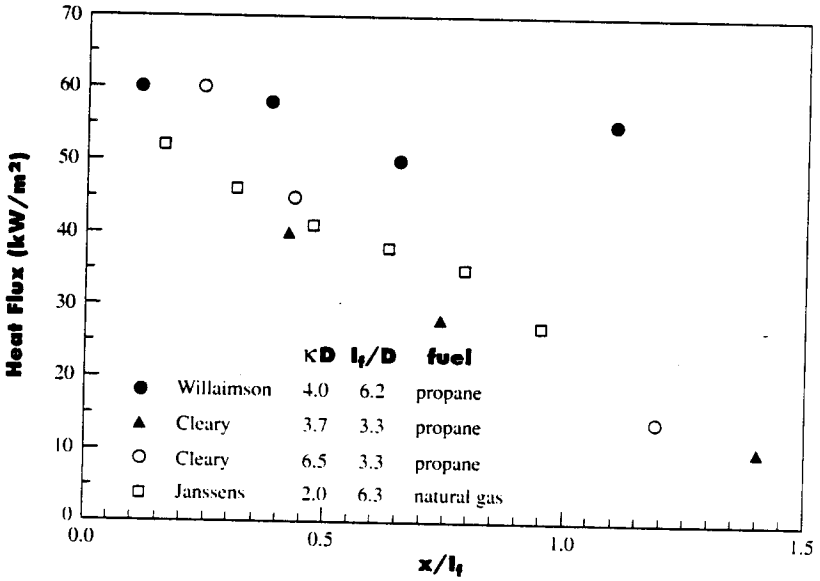

Figure 9. Corner heat flux (effect of fuel). Data from Williamson *et al.*[11] and from Janssens and Tran.[10]

zero. In addition, there is an implied family of curves increasing in heat flux as x/l_f decreases (see Figure 7).

Figure 9 shows the effect of fuel in terms of the κD parameter. For a fixed l_f/D, an increase in κD causes an increase in the heat flux, as would be expected by considerations of flame radiation. More data are needed to establish accurate quantitative correlations.

Case 3: Window Flames

Oleszkiewicz[13] studied the heat flux to an external wall above a window flame. He generated the window flame from a propane burner in a compartment and induced the air supply by natural convection through the same window. Window size and fuel supply rate was varied. The heat flux was measured at several positions along the centerline above the window. Oleszkiewicz[14] recorded the average window flame length, assumed to be based upon the tip. The average window flame length was also computed from a correlation based on the window plume study by Yokoi[16] and the work of Thomas and Law.[17]

Figure 10 shows the geometry of the window flame experiments and the notation. The equivalent window radius is given by Equation (8). Following the analysis of Yokoi[16] and of Thomas and Law,[17] and noting that the case of the wall above the window corresponds to the "no wall" case with $n=W_0/2H_0 \approx 1$ as presented by Yokoi,[16]

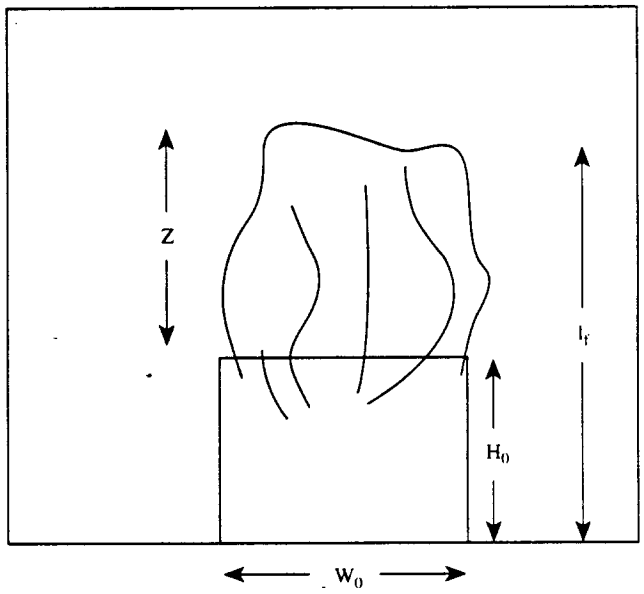

Figure 10. Window flame configuration.

$$\frac{z + H_0}{r_0} = \frac{B}{\Theta} \tag{15}$$

where Θ is a dimensionless temperature given by

$$\Theta = \frac{\Delta\theta\, r_0^{5/3}}{\sqrt[3]{\frac{\dot{Q}^2\theta_0}{c_p^2\rho^2 g}}} \tag{16}$$

and we select B=2.[17] For computing flame height, we select Θ_0 = 290K, ρ=0.45 kg/m^3 at 500°C, per Thomas and Law,[17] c_p=1.0 kJ/kg K, and g=9.81 m/s^2. It is specified that $\Delta\theta$ at the flame tip=520°C. With the constants specified, Equation (16) therefore becomes

$$\Theta = 98.9\frac{r_0^{5/3}}{\dot{Q}^{2/3}} \tag{17}$$

Noting that $D=2r_0$, we finally obtain for $l_f=z+H_0$

$$l_f = 0.0321\left(\frac{\dot{Q}}{D}\right)^{2/3} \tag{18}$$

with l_f and D in m and $\dot{Q}$ in kW.

In this analysis, $\dot{Q}$ is taken as the energy release rate based on the fuel supply rate. However, Yokoi's formulation requires the energy flow rate at the window. Hence, heat losses to the room are not included. If the heat losses to the room were estimated and subtracted from the various $\dot{Q}$ values, this dilemma could be addressed. The data and calculated flame heights are presented in Table 3. Figure 11 shows $\dot{q}''$ measured by Oleszkiewicz[14] as a function of x/l_f for different ranges of l_f/D, based on calculated flame heights. The data of solid square symbols falling above the trend are due primarily to the 2.6-m-wide-by-1.37-m-high window at the highest energy release rate of 10.3 MW. In general, it appears that some combination of l_f/D and κD are responsible for the scatter. The measured flame heights from Oleszkiewicz[14] are plotted against calculated flame heights using Equation (18) in Figure 12. This suggests that the calculated values are roughly double the measured flame heights. Hence, a value of B=1 would have been a better choice. This value is more consistent with 1.3 suggested by Thomas and Law[17] for their data with compartment heat losses.

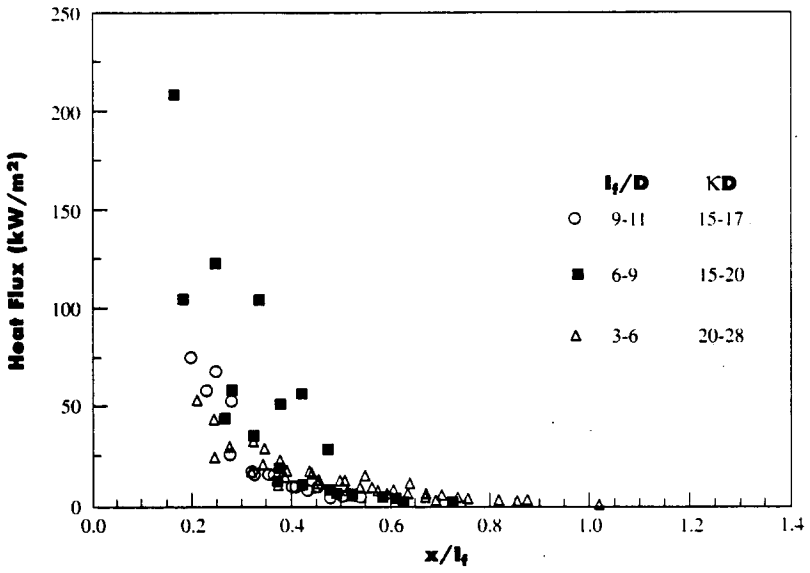

Figure 11. Flame heat flux above a window based on calculated flame height.

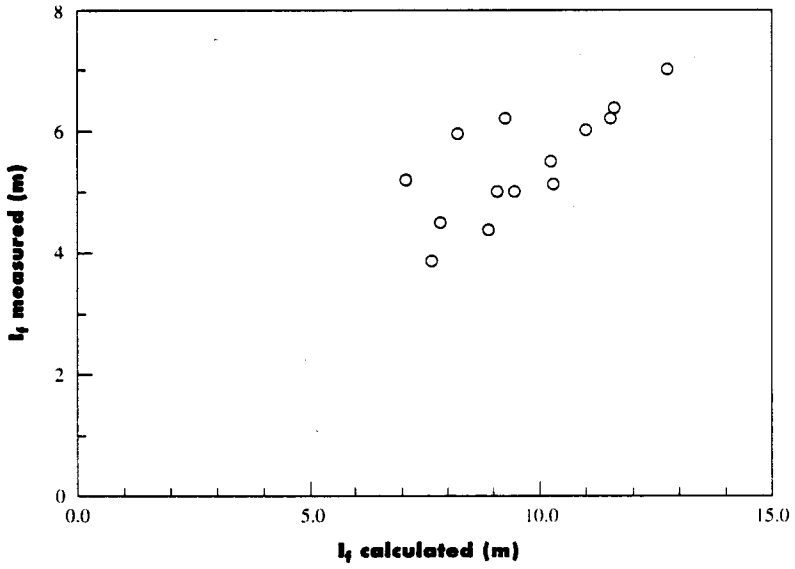

Figure 12. Window flame length (measured versus predicted from Yokoi[16]).

Finally, in Figure 13, we plot $\dot{q}''$ versus x/l_f using measured flame heights. This final plot shows more contrast among the different l_f/D ranges, but no significant differences from Figure 11.

Discussion

The preliminary correlations for flame heat flux show that the flux distribution can be reasonably scaled with flame length. Specifically, the heat flux distribution is similar with distance from the source normalized with flame length. In the case of line fires or wall fires, the maximum flame heat flux is 30 kW/m^2 for flames as high as 2 m. For square burner flames against a wall or in a corner, however, the incident flux was recorded as high as 80 kW/m^2 along the centerline and 120 kW/m^2 closer to the corner/wall intersection. This is apparently due to the flame thickness induced by the burner dimension D and to the reradiation from the wall surfaces. Furthermore, these data are for a limited range of conditions, so that these fluxes are anecdotal. For corner fires, the parameter l_f/D appears to have a stronger effect on increasing the heat flux over a greater distance x/l_f as indicated by Figure 7. The parameter κD enhances heat flux in a similar manner, as indicated by Figure 9.

The heat flux correlation for the window flames does not appear to be as successful, even when measured flame lengths are used. However, these heat fluxes are consid-

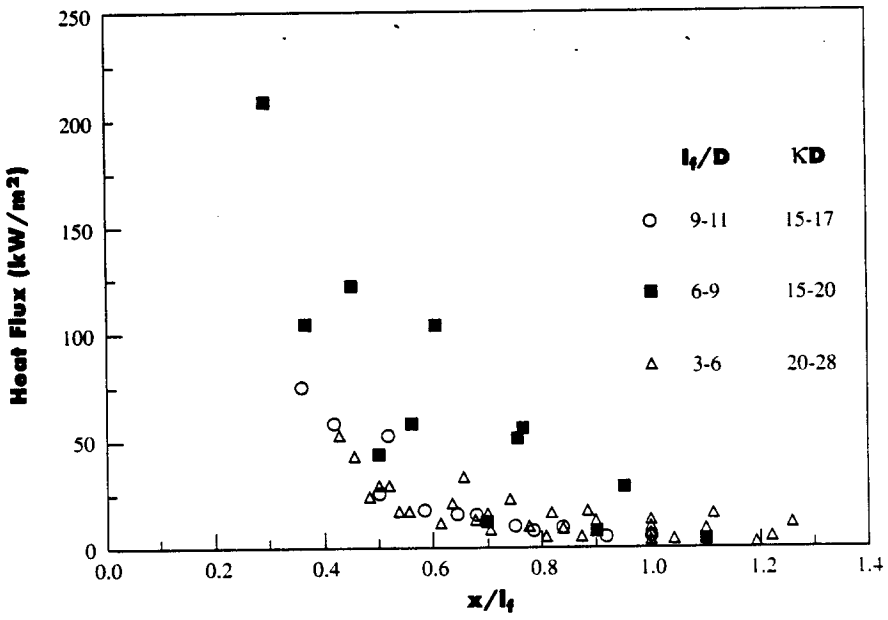

Figure 13. Flame heat flux above a window based on measured flame height.

erably higher than wall fires, and they range up to 200 kW/m^2. The geometry of the window flame may not be fully accounted for when using the equivalent window radius r_0. Moreover, the Yokoi correlation for flame height does not appear to fit the data for at least three points.

The wide range of heat fluxes reported for these configurations make it critical to establish more definitive predictive methods. This is particularly necessary when modeling standard tests that incorporate a burner as the ignition source. The heat flux clearly depends on the energy release rate selected for the burner, its size, and the type of gaseous fuel used. Moreover, the burning rate of a particular wall material and its contribution to its heat flux environment is the key element in assessing fire hazard. Without a method to predict these heat fluxes, it will not be possible to accurately link small-scale material fire data to realistic fire scenarios. It is apparent from the limited data available that more systematic experiments are needed. If more data are developed, we might seek more general analytical correlations that could be applied with confidence. The current presentation can only be used for estimates over ranges of the variables represented by the data. It would be risky to extrapolate for these limited results.

Nomenclature

B	constant
C	constant
D	characteristic fire dimension: side of square burner, equivalent window diameter
H_o	window height
Q	energy
Q^*	$Q / \rho_\infty c_p T_\infty \sqrt{gD^{5/2}}$
T	temperature
W_o	window width
W	width of line burner or wall flame
c_p	heat capacity
g	gravitational constant
h	heat transfer coefficient
l_f	flame height
l_m	mean beam length
q	heat transfer
r_0	equivalent window radius
x	vertical distance
y	horizontal distance
z	flame height from top of window
δ	boundary layer thickness
Δ	difference

θ	temperature
Θ	dimensionless temperature
κ	flame absorption coefficient
ρ	density
σ	Stefan-Boltzmann constant

Superscripts

.	per unit time
"	per unit area
'''	per unit volume

Subscripts

c	convection
f	flame
r	radiation
∞	ambient
o	initial

References

1. Orloff, L., de Ris, J., and Markstein, G.M., *Upward Turbulent Fire Spread and Burning of Fuel Surface*, Fifteenth Symposium (International) Combustion, Combustion Institute, Pittsburgh, 1982, pp. 885-895.

2. Orloff, L., and de Ris,J., "Froude Modeling of Pool Fires," 19th Symposium (International) Combustion, Combustion Institute, Pittsburgh, 1982, pp. 885-895.

3. Ahmad, T., and Faeth, G.M., "Turbulent Wall Fires," *17th Symposium (International) on Combustion*, The Combustion Institute, 1979, pp. 1149-1160.

4. Quintiere, J.G., Harkleroad, M., and Hasemi, Y., "Wall Flames and Implications for Upward Flame Spread," *Combustion Science and Technology*, Vol. 48, 1986, pp. 191-222.

5. Harkleroad, M., "Ignition and Flame Spread Measurements of Aircraft Lining Materials," National Bureau of Standards, *NBSIR 88-3773*, 1988.

6. Mitler, H., "Algorithm for the Mass-Loss Rate of a Burning Wall," *Proceedings of the 2nd International Symposium on Fire Safety Science*, ed. P. Pagni and C. Grant, Hemisphere Publishing, N.Y., 1989, pp. 179-188.

7. Babrauskas, V., Lawson, J.R., Walter, W.D., and Twilley, W.H., "Upholstered Furniture Heat Release Rates Measured with a Furniture Calorimeter," National Bureau of Standards, *NBSIR 82-2604*, 1982.

8. Babrauskas, V., and Krasny, J., "Fire Behavior of Upholstered Furniture," National Bureau of Standards, *NBS Monograph 173*, 1985.

9. Janssens, M., "Fundamental Thermophysical Characteristics of Wood and Their Role in Enclosure Fire Growth," University of Gent (Belgium), September 1991.

10. Janssens, M., and Tran, H.C., "Modeling the Burner Source Used in ASTM Room Fire Test," to be submitted for publication, 1992.

11. Williamson, R.B., Revenaugh, A., and Mowrer, F.W., "Ignition Sources in Room Fire Tests and Some Implications for Flame Spread Evaluation," *Proceedings of the Third International Symposium on Fire Safety Science*, ed. G. Cox and B. Langford, Elsevier Applied Science, London, 1991.

12. Cleary, T., unpublished data, National Institute of Standards and Technology, 1989.

13. Oleszkiewicz, I., *Heat Transfer from a Window Fire Plume to a Building Facade*, American Society of Mechanical Engineers, HTD-Vol. 123, Book No. H00526, 1989.

14. Oleszkiewicz, I., private communication on flame heights, January 29, 1992.

15. Tien, C.L., Kee, K. Y., and Stretton, A.J., "Radiation Heat Transfer," *SFPE Handbook of Fire Protection Engineering*, P. DiNenno, editor-in-chief, National Fire Protection Association, Boston, Mass., 1988.

16. Yokoi, S., "Study on the Prevention of Fire Spread Caused by Hot Upward Current," Building Research Institute (Japan), *Report No. 34*, 1960.

17. Thomas, P.H., and Law, M., "The Projection of Flames from Buildings on Fire," *Fire Prevention Science and Technology*, No. 10, 1974, pp. 19-26.

18. McCaffrey, B.J., "Purely Buoyant Diffusion Flames: Some Experimental Results," National Bureau of Standards, *NBSIR 79-1910*, 1979.

19. Tu, K.M., and Quintiere, J.G., "Wall Flame Heights with External Radiation," *Fire Technology*, Vol. 23, No. 3, pp. 195.

20. Hasemi, Y., "Experimental Wall Flame Heat Transfer Correlations for the Analysis of Upward Wall Flame Spread," *Fire Science and Technology*, Vol. 4, No. 2 pp. 75-90, 1984.

21. Kulkarni, A.K., "Radiative and Total Heat Feedback from Flames to Surface in Vertical Wall Fires," Experimental Heat Transfer, Vol. 3, pp. 411-426, 1990.

22. Hasemi, Y., and Tokunaga, T., "Some Experimental Aspects of Turbulent Diffusion Flames and Buoyant Plumes from Fire Sources Against a Wall and in a Corner of Walls," *Combustion Science and Technology*, Vol. 40, 1984, pp. 1-17.